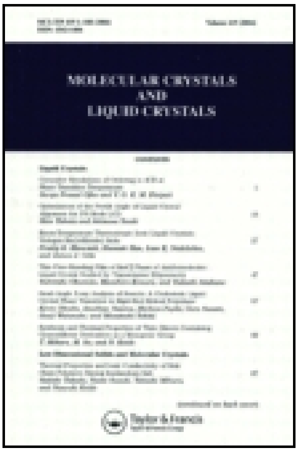

Molecular Crystals and Liquid Crystals
Publication details, including instructions for authors and subscription information:
http://www.tandfonline.com/loi/gmcl20

Liquid-Crystal Tunable Long-Range Surface Plasmon Polariton Directional Coupler

Dimitrios C. Zografopoulos [a] & Romeo Beccherelli [a]
[a] Consiglio Nazionale delle Ricerche, Istituto per la Microelettronica e Microsistemi (CNR-IMM) , Rome , Italy
Published online: 02 Apr 2013.

Mol. Cryst. Liq. Cryst., Vol. 573: pp. 70–76, 2013

ISSN: 1542-1406 print/1563-5287 online
DOI: 10.1080/15421406.2013.763339

Liquid-Crystal Tunable Long-Range Surface Plasmon Polariton Directional Coupler

DIMITRIOS C. ZOGRAFOPOULOS* AND ROMEO BECCHERELLI

Consiglio Nazionale delle Ricerche, Istituto per la Microelettronica e Microsistemi (CNR-IMM), Rome, Italy

A tunable plasmonic directional coupler is proposed based on the electro-optical control of a nematic liquid-crystal layer placed above two side-coupled gold stripe waveguides. It is shown that by proper adjustment of the structural parameters and the control voltage, the coupling length of the structure and the effective modal index of the individual waveguides can be tuned, allowing for the design of electro-optical liquid-crystal plasmonic directional coupler switches.

Keywords Directional couplers; nematic liquid crystals, optical interconnects; plasmonic waveguides

Introduction

Significant scientific attention has been drawn in the last years in the field of plasmonics, which, among numerous other applications, has also been proposed as an emerging platform for the development of high-bandwidth, reduced-size, and potentially low power consumption integrated photonic circuitry [1]. In this context, surface plasmon polaritons (SPP), light waves excited at the interface between a dielectric and a metal, silver, or gold being typical yet no single choices [2], have been widely exploited in the design of numerous waveguides that provide a wide range of optical properties, such as light confinement, which has been pushed below the subwavelength limit of conventional dielectric photonics. Among these options, light guidance in thin metal stripes presents acceptably low dumping losses, excellent mode-matching with single-mode fibers, and the ability to directly address the optical field via current injection or voltage application, making them a promising solution for interchip interconnects [3]. Following the early demonstration of passive waveguides and components, for example, power splitters and grating filters, active components required for light routing in real applications, such as variable attenuators, Mach–Zehnder interferometers and directional coupler switches (DCSs) were investigated, based on the thermal tuning of the modal properties of the fundamental long-range (LR) guided SPP mode, via the control of the refractive index of the surrounding materials [4–6].

In this work, we propose and analyze a long-range surface plasmon polariton (LRSPP) DCS, which is based on a different approach, namely, the electro-optical tuning of a

*Address correspondence to Dimitrios C. Zografopoulos, Consiglio Nazionale delle Ricerche, Istituto per la Microelettronica e Microsistemi (CNR-IMM), Rome, Italy. E-mail: dimitrios.zografopoulos@artov.imm.cnr.it

nematic liquid crystal (NLC) layer introduced above the plasmonic guiding area [7,8]. It is demonstrated that the switching of the LC molecules can properly modify the optical properties of side-coupled transverse magnetic-polarized gold stripe waveguides and tune the response of the coupler. At first, the numerical studies involve the rigorous solution of the LC molecular orientation profile [8,9], by solving for the coupled elastic and electrostatic underlying physical problems. Then, the derived LC molecular orientation profiles are used to obtain the optical dielectric tensor profile, which is fed into a finite element-method analysis [10] that finally yields the structure's optical response. It is demonstrated that by proper design, the proposed device can operate as a DCS, electro-optically controlled by the value of the applied voltage. Such tunable LC-LRSPP components are envisaged as ultralow power consumption building elements in integrated plasmonic circuitry.

LC-LRSPP Directional Coupler Switches

The LC-tunable plasmonic directional couplers under investigation are based on the LC-LRSPP waveguide shown in Fig. 1. A gold stripe, whose complex refractive index equals $n_{Au} = 0.55 - j11.5$ [11], is embedded in a polymer with a refractive index $n_p = 1.505$ and a relative permittivity $\varepsilon_p = 2.5$. In the superstratum, a planar LC cell is formed, infiltrated by the common nematic material E7, which is characterized by relative ordinary and extraordinary permittivities equal to $\varepsilon_{per} = 5.3$, $\varepsilon_{par} = 18.6$, respectively, and elastic constants $K_{11} = 10.3$ pN, $K_{22} = 7.4$ pN, and $K_{33} = 16.48$ pN [12]. Its ordinary and extraordinary refractive indices equal $n_o = 1.5024$ and $n_e = 1.697$ [13]. The structure is sandwiched between two poly(methyl methacrylate) layers with $n_{\mathrm{PMMA}} = 1.493$, $\varepsilon_{\mathrm{PMMA}} = 3.9$, which prevent light from coming to contact with the ITO electrodes, characterized by $n_{\mathrm{ITO}} = 1.27 - j0.12$. The upper ITO electrode serves for the application of the control voltage V, while the lower one, as well as the Au stripe, is grounded. All material indices refer to the telecom wavelength of 1.55 μm. The structure's geometrical parameters, that is, thickness of the various layers and the dimensions of the Au stripe, are set to $h_{\mathrm{LC}} = 5\ \mu$m, $h_{\mathrm{ITO}} = 100$ nm, $h_{\mathrm{sub}} = 10\ \mu$m, $h_{\mathrm{buf}} = 2\ \mu$m, $h_{\mathrm{PMMA}} = 3\ \mu$m, $w_{\mathrm{Au}} = 5\ \mu$m, and $t_{\mathrm{Au}} = 15$ nm, with reference to the definitions of Fig. 1.

In absence of applied voltage the LC molecules are aligned along the z-axis, strongly anchored at the LC/polymer interface. In that state, the index sensed by the TM-polarized

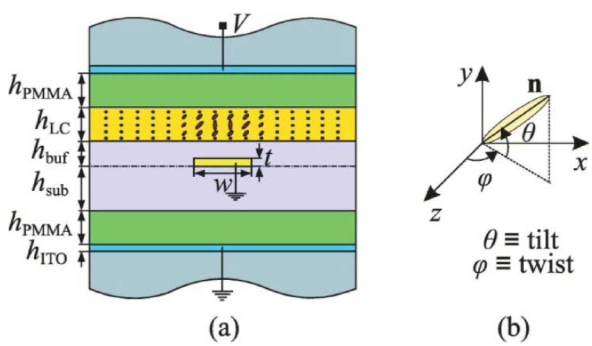

Figure 1. (a) Layout of the proposed liquid-crystal/LR plasmonic waveguide and definition of the relevant structural parameters. (b) Definition of the coordinate system and the nematic director via the tilt (θ) and twist (φ) angles describing the local orientation of the LC molecules.

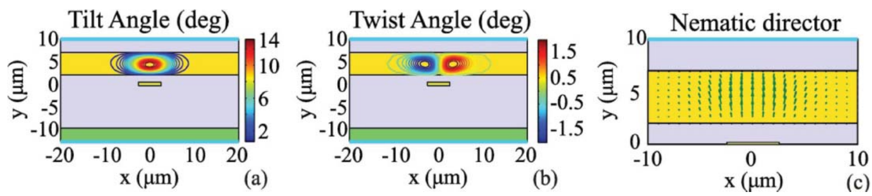

Figure 2. Profile of the tilt (a) and twist (b) angles, as well as (c) distribution of the nematic director for an applied voltage of 3.1 V for the hybrid LRSPP/LC waveguide of Fig. 1.The twist angle obtains much lower values than the tilt one and it has a negligible effect in the waveguide's optical properties.

LRSPP mode in the LC layer equals $n_o < n_p$, and light is guided via the plasmonic stripe, as it is prohibited to enter into the lower index LC zone. When V exceeds the Fréederickz transition threshold, the LC molecules tilt in the area above the Au stripe as demonstrated in Fig. 2, where the tilt, twist angle and the nematic director distribution are plotted for $V = 3.1$ V. As a consequence, a high refractive index zone is created for TM-polarized light, which leads to light leakage into the dielectric waveguide formed inside the LC-layer by the tilted molecules. By controlling the value of the applied voltage, the modal profile and the effective modal index can be tuned as shown in Fig. 3.

Figure 4 shows the layout of the proposed DCS, which is formed by side coupling two of the individual hybrid LRSPP/LC waveguides. The top ITO electrode is patterned in order to separately address each waveguide and control the optical properties of the coupler. The LC-switching dynamics in the coupled configuration are qualitatively similar to the single waveguide case, as evidenced in Fig. 5 where the molecular orientation is studied for an applied voltage $V_1 = V_2 = 3.1$, that is, identical to the case investigated in Fig. 2. As expected, by properly selecting different values of V_1 and V_2, the level of switching above each waveguide can also be controlled.

At the rest state, the coupling length L_c, namely, the propagation distance at which complete power transfer is achieved from the excited and the coupled waveguide can be

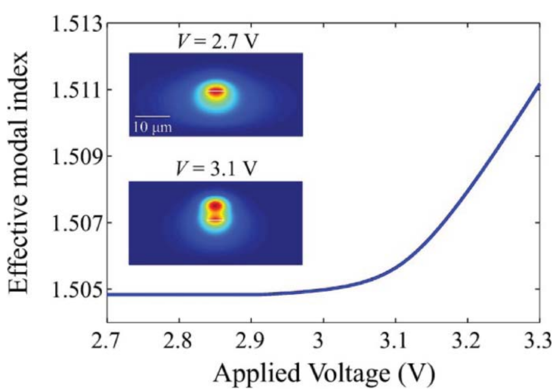

Figure 3. Dependence of the effective modal index of the fundamental mode supported by the hybrid waveguide under study versus applied voltage. For voltage values below a threshold $V_{th} \sim 2.9$ V, the LC molecules remain aligned with the z-axis and a purely LR-SPP mode fundamental mode is supported. For higher values of V, part of the optical power escapes into the high-index LC-dielectric waveguide formed above the metal stripe, raising the effective modal index.

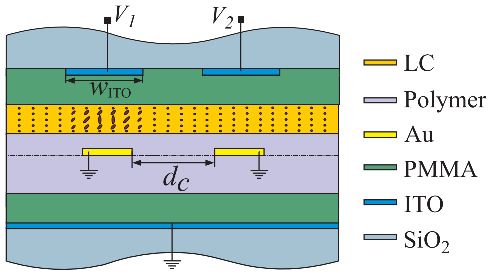

Figure 4. Layout of the proposed LR-SPP/LC directional coupler. Two structurally identical waveguides are side coupled at a separation distance d_c and controlled by individual voltages V_1, V_2, applied by properly patterned ITO stripes.

calculated according to $L_c = 0.5\lambda/\Delta n$, where Δn is the difference between the effective modal index of the symmetric and antisymmetric supermodes supported by the coupler [14]. Figure 6(a) shows the effective modal indices of both supermodes as a function of the separation d_c between the two waveguides, assuming for simplicity $w_{ITO} = w_{Au}$, as well as their optical power profile for $d_c = 5$ μm. The corresponding coupling length, as calculated at Fig. 6(b), lies in the few mm range, typical of LRSPP directional couplers [15], and exponentially increases as the two waveguides are placed at a greater distance.

Next, we fix the waveguide separation to 5 μm, and investigate into the dynamically tunable properties of the coupler. In a first approach, we consider that the same voltage is applied to both waveguides. Since $V_1 = V_2 = V$, the structure retains its symmetry and the two waveguides remain identical regardless of the applied voltage. Nevertheless, above the LC-switching threshold the effective modal indices of the supported supermodes change and, consequently, the coupling length L_c is modified. This effect is studied in Fig. 7(a) where L_c is plotted as a function of V. It can be observed that as the applied voltage increases, the corresponding coupling length is reduced compared to that in the rest state, which was found equal to $L_c(V = 0) = 1.51$ mm. As V is further increased, there exists a critical value V_{cr} for which $L_c(V_{cr}) = 0.5L_c(V = 0)$, which in the case under study was found equal to 2.98 V. Operation at that voltage allows for the switching of the exit ports of the directional coupler compared to the rest state, as optical power is transferred back to the input waveguide if the total device length is selected as $L_c(V = 0) = 1.53$ mm. According to the coupled mode theory (CMT) [14], power exchange between the excited (BAR), and

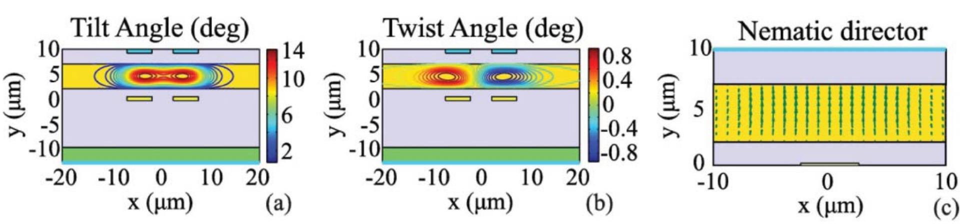

Figure 5. Profile of the tilt (a) and twist (b) angles, as well as (c) distribution of the nematic director for an applied voltage of $V_1 = V_2 = 3.1$ V for the hybrid LR-SPP/LC directional coupler of Fig. 4. Results can be directly compared to those of Fig. 2: two high-tilt zones are formed above the side-coupled Au stripes, with a maximum value of 14° in their central part.

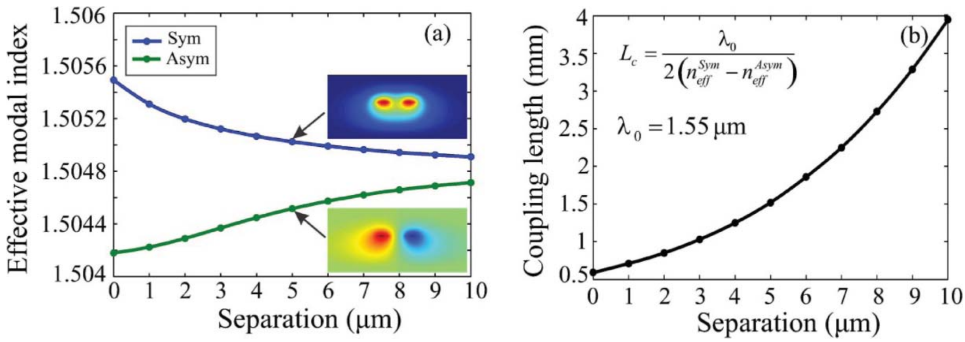

Figure 6. (a) Effective modal indices of the fundamental symmetric and asymmetric supermodes supported by the proposed coupler for different values of the separation d_c between the two side-coupled waveguides, in the absence of applied voltage ($V_1 = V_2 = 0$). (b) Corresponding values of the coupling length L_c of the structure.

coupled (CROSS) waveguide along the propagation distance z is given by

$$P_{BAR} = \cos^2(\kappa z), \quad P_{CROSS} = \sin^2(\kappa z) \tag{1}$$

where the coupling coefficient κ equals $\kappa = \pi/(2L_c)$. Figure 7(b) shows the power transfer when the coupler operates selectively between the two control states $V = 0$ and $V = V_{cr}$. At $V = 0$ the optical power is coupled to the cross waveguide at the exit of the coupler at $z = L_c(V = 0) = 1.51$ mm of the component, while at $V = V_{cr}$ the output state is switched, since the coupling length is reduced to half of the component's length. It should be stated that in this approach the waveguide's losses are not taken into account. For the material and structural parameters here investigated, these are estimated in the order of few dB/cm [7,8], which implies sub-dB insertion losses for the proposed device, which are acceptable in most applications.

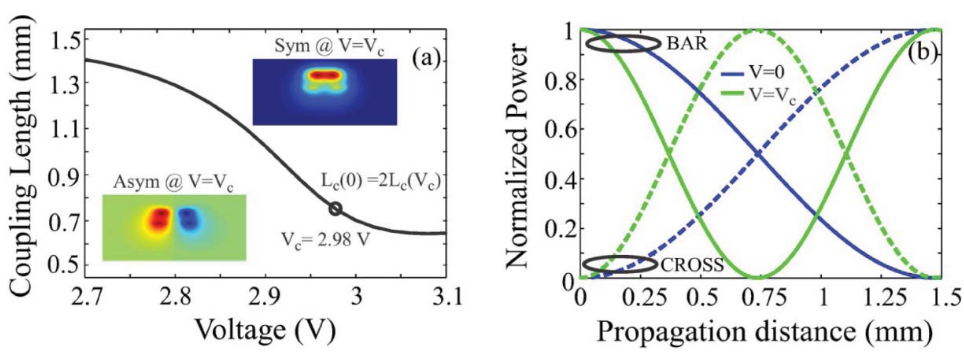

Figure 7. (a) Coupling length for $d_c = 5$ μm calculated for values of the common applied voltage $V = V_1 = V_2$ up to 3.1 V. At the critical value $V_{cr} = 2.98$ V the coupling length becomes half of the corresponding L_c in the absence of applied voltage. (b) Power transfer in the bar and cross output state along propagation. At $L_{c,0} = 1.51$ mm voltage-controlled switching of the exit state is achieved for operation between $V = 0$ and V_{cr}.

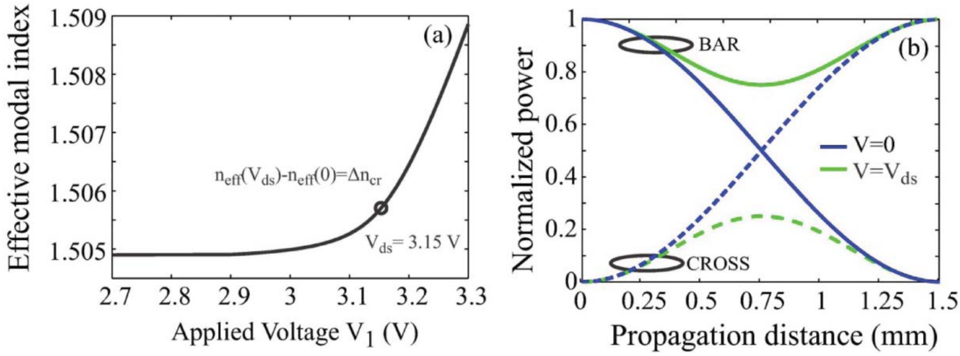

Figure 8. (a) Effective model index of the left waveguide calculated as a function of the applied voltage V_1, while $V_2 = 0$. The realistic LC molecular orientation profiles corresponding to the coupled structure were used for the calculations. The critical value Δn_{cr} required for desynchronization of the coupler is found when the applied voltage V_1 equals $V_{ds} = 3.15$ V. (b) Power transfer in the bar and cross output state along the propagation distance, estimated via the CMT for operation at the limit values $V_1 = V_2 = 0$ and $V_1 = V_{ds}$, $V_2 = 0$. For a component length equal to $L_c(V = 0) = 1.51$ mm, switching of the exit state is achieved when operating between the control values $V_1 = 0$ and $V_1 = V_{ds}$.

In a complementary approach toward the design of a LC-LRSPP-DCS, we consider the case where only one of the two waveguides is electro-optically addressed, namely $V_1 = V$, $V_2 = 0$, with respect to the layout of Fig. 4. This condition lifts the symmetry of the structure, and the two waveguides are no longer identical. As V_1 is increased, the left waveguide follows the transition from a plasmonic to hybrid-LC waveguide, while the right one remains unaffected. Figure 8(a) shows the tuning of the individual mode in the left waveguide, that is, in the absence of the right one, nevertheless calculated using the nematic director profiles derived from the solution of the electrostatic problem in the coupled structure, in order to account for the realistic nematic molecular configurations. A similar study showed no significant variation of the effective modal index of the right waveguide, which corresponds to $V_2 = 0$.

As predicted by the CMT, when the two waveguides are desynchronized by a difference in their propagation constants $\Delta\beta = k_0\Delta n$, power transfer in the two arms of the coupler is given by

$$P_{\mathrm{BAR}} = 1 - P_{\mathrm{CROSS}}, \quad P_{\mathrm{CROSS}} = \frac{k^2}{k^2 + \frac{\Delta\beta^2}{4}} \sin^2\left(\sqrt{k^2 + \frac{\Delta\beta^2}{4}} z\right). \tag{2}$$

When $\Delta\beta$ obtains the critical value $\Delta\beta_{cr} = \sqrt{3}\pi/L_c$, or, equivalently, $\Delta n_{cr} = 0.5\sqrt{3}(\lambda/L_c)$, the exit of the coupler at $L = L_c$ is switched, as shown in Fig. 8(b). For the case studied the voltage that provides the Δn_{cr} for the desynchronization of the two waveguide arms was been found equal to $V_{ds} = 3.15$ V. The total device length remains in this case as well equal to $L_c(V = 0) = 1.51$ mm.

As in all photonic devices based on the electro-optical tuning of nematic liquid crystals, the response times of the proposed components is expected to lie in the ms range, which is sufficient for light routing and switching in interconnect applications [16]. Furthermore, given that LC switching involves a capacitive operation, the total power consumption in the presented geometries can be estimated as $P \approx CV^2f$, C being the capacitance and f

the LC-driving frequency, typically in the range 1∼10 kHz. This results in a submicrowatt value, which is orders of magnitude lower than the milliwatt range of thermo-optic LRSPP tunable components [4–6].

Conclusions

Novel functional LRSPP tunable directional couplers based on the electro-optical control of a nematic liquid-crystal layer formed in the superstratum of the plasmonic Au stripe waveguides were designed and theoretically investigated. It has been shown that by proper selection of the applied control voltages, the optical properties of the side-coupled waveguides, as well as of the coupler structure can be extensively tuned. This tunability can be exploited for the design of DCSs, which are proposed as low-power consumption functional elements in plasmonic circuitry for optical interconnects.

Acknowledgments

This work was supported by the Marie-Curie Intra-European Fellowship ALLOPLASM (FP7-PEOPLE-2010-IEF-273528), within the 7th European Community Framework Programme.

References

[1] Ebbesen, T. W., Genet, C., & Bozhevolnyi, S. I. (2008). *Phys.Today*, *61*, 44.
[2] Naik, G. V., Schroeder, J. L., Ni, X., Kildishev, A. V., Sands, T. D., & Boltasseva, A., (2012). *Opt. Mater. Express*, *2*, 478.
[3] Berini, P. (2009). *Adv. Opt. Photon.*, *1*, 484.
[4] Nikolajsen, T., Leosson, K., Bozhevolnyi, S. I. (2005). *Opt. Commun.*, *244*, 455.
[5] Gagnon, G., Lahoud, N., Mattiussi, G. A., & Berini, P. (2006). *J. Lightwave Technol.*, *24*, 4391.
[6] Nikolajsen, T., Leosson, K., & Bozhevolnyi, S. I. (2004). *Appl. Phys. Lett.*, *85*, 5833.
[7] Zografopoulos, D. C., & Beccherelli, R. (2012). *Plasmonics*, DOI: 10.1007/s11468-012-9440-7.
[8] Zografopoulos, D. C., Beccherelli, R., Tasolamprou, A. C., & Kriezis, E. E. (2012). *Photonics Nanostruct.*, DOI: 10.1016/j.photonics.2012.08.004.
[9] Bellini, B., & Beccherelli, R. (2009). *J. Phys. D: Appl. Phys.*, *42*, 045111.
[10] COMSOL Multiphysics, v. 4.2, www.comsol.com.
[11] Johnson, P. B., & Christy, R. W. (1972). *Phys. Rev. B*, *6*, 4370.
[12] Strömer, J. F., Raynes, E. P., & Brown, C. V. (2006). *Appl. Phys. Lett.*, *88*, 051915.
[13] Li, J., Wu, S., Brugioni, S., Meucci, R., & Faetti, S. (2005). *J. Appl. Phys.*, *97*, 071501.
[14] Vassallo, C., *Optical Waveguide Concepts*. Elsevier: Amsterdam, 1991.
[15] Srivastava, T., & Kumar, A. (2010). *Appl. Opt.*, *49*, 2397.
[16] Zografopoulos, D. C., Asquini, R., Kriezis, E. E., d'Alessandro, A., & Beccherelli, R. (2012). *Lab Chip*, *12*, 3598.